Available online at www.sciencedirect.com
SCIENCE DIRECT®
Remote Sensing of Environment 85 (2003) 304–315
Remote Sensing of Environment
www.elsevier.com/locate/rse

A new parameterization of canopy spectral response to incident solar radiation: case study with hyperspectral data from pine dominant forest

Yujie Wang[a,*], Wolfgang Buermann[a], Pauline Stenberg[b], Heikki Smolander[c], Tuomas Häme[d], Yuhong Tian[a], Jiannan Hu[a], Yuri Knyazikhin[a], Ranga B. Myneni[a]

[a] Department of Geography, Boston University, Boston, MA 02215, USA
[b] Department of Forest Ecology, University of Helsinki, FIN-00014 Helsinki, Finland
[c] Finnish Forest Research Institute, Suonenjoki Research Station, FIN-77600 Suonenjoki, Finland
[d] VTT Automation, Remote Sensing Group, FIN-02044 VTT, Finland

Received 27 March 2002; received in revised form 15 December 2002; accepted 15 December 2002

Abstract

A small set of independent variables generally seems to suffice when attempting to describe the spectral response of a vegetation canopy to incident solar radiation. This set includes the soil reflectance, the single-scattering albedo, canopy transmittance, reflectance and interception, the portion of uncollided radiation in the total incident radiation, and portions of collided canopy transmittance and interception. All of these are measurable; they satisfy a simple system of equations and constitute a set that fully describes the law of energy conservation in vegetation canopies at any wavelength in the visible and near-infrared part of the solar spectrum. Further, the system of equations specifies the relationship between the optical properties at the leaf and the canopy scales. Thus, the information content of hyperspectral data can be fully exploited if these variables can be retrieved, for they can be more directly related to some of the physical properties of the canopy (e.g. leaf area index). This paper demonstrates this concept through retrievals of single-scattering albedo, canopy absorptance, portions of uncollided and collided canopy transmittance, and interception from hyperspectral data collected during a field campaign in Ruokolahti, Finland, June 14–21, 2000. The retrieved variables are then used to estimate canopy leaf area index, vegetation ground cover, and also the ratio of direct to total incident solar radiation at blue, green, red, and near-infrared spectral intervals.

Keywords: Vegetation canopy; Parameterization; Spectra

1. Introduction

About 30% of the earth is covered by land and much of this is vegetated. Terrestrial vegetation impacts climate by playing a key role in various processes of energy, mass, and momentum exchanges (Bonan, 1996; Dickinson, Henderson-sellers, Kennedy, & Wilson, 1986; Foley, Levis, Prentice, Pollard, & Thompson, 1998; Sellers et al., 1997). It has been recognized that changes in vegetation affect climate to an extent comparable to forcing resulting from changes in atmospheric composition, ocean circulation, and orbital perturbations (Pielke et al., 1998). Knowing how much of the short-wave radiation is absorbed by the canopy, understory, and the ground helps better predict the near-surface climate (Buermann, Dong, Zeng, Myneni, & Dickinson, 2001). Therefore, it is important to identify and characterize variables that govern energy conservation in vegetation canopies; that is, the partitioning of incident radiation into its canopy, understory, and ground-absorbed components.

Remotely sensed hyperspectral data offer considerable potential for obtaining information about the earth surface. There is a considerable body of literature on the use of hyperspectral data for small target detection, material identification, discrimination among very similar classes, and estimation of biochemical or geophysical parameters, for which a dense sampling of a selected range of the electromagnetic spectrum is especially diagnostic (Baret & Jacquemoud, 1994; Blackburn, 1998; Broge & Leblanc, 2000;

* Corresponding author. Goddard Earth Sciences and Technology Center, University of Maryland, Baltimore County, Rm. 3.002, 1450 South Rolling Rd., Baltimore, MD 21227, USA. Tel.: +1-410-455-8807; fax: +1-410-455-8806.
E-mail address: yujie@umbc.edu (Y. Wang).

0034-4257/03/$ - see front matter © 2003 Elsevier Science Inc. All rights reserved.
doi:10.1016/S0034-4257(03)00009-9

Lewis, Jooste, & de Gasparis, 2001; Serpico & Bruzzone, 2001; Thenkabail, Smith, & Paue, 2000; Zarco-Tejada, Miller, Noland, Mohammed, & Sampson, 2001).

Many studies have investigated the interaction of solar radiation with vegetation canopies by the use of models. Most of them are aimed at examining the spectral reflectance of vegetation and the relationship to a particular chemical or biophysical process (Broge & Leblanc, 2000; Thenkabail et al., 2000; Zarco-Tejada et al., 2001). An alternate method is to first relate canopy reflectances to parameters responsible for the distribution of solar radiation in vegetation canopies and further relate these to variables characterizing canopy structure and biochemical properties (e.g. leaf area index, chlorophyll content, etc.). This concept underlies the operational algorithm for the retrieval of global leaf area index and fraction of absorbed photosynthetically active radiation developed for the moderate resolution spectroradiometer (MODIS) and multiangle imaging spectroradiometer (MISR) instruments of the Earth Observing System Terra mission (Knyazikhin, Martonchik, Myneni, Diner, & Runing, 1998).

Three factors determine the radiative regime in vegetation canopies (Ross, 1981): the architecture of an individual plant and the entire canopy, which are wavelength independent; optical properties of vegetation elements (leaves, stems) and the soil; and spectral composition of the incident radiation field. Solar radiation transmitted and absorbed by vegetation canopy can be described by expressions that relate canopy transmittance and absorptance at an arbitrary wavelength to transmittances and absorptances at all other wavelength in the solar spectrum (Knyazikhin et al., 1998; Panferov et al., 2001; Shabanov et al., in preparation). These relationships require the single-scattering albedo and two canopy structure-specific variables that do not depend on leaf optical properties. These structural variables are portions of collided radiation in total transmitted and intercepted radiation normalized by the single-scattering albedo (Shabanov et al., in preparation). They accurately specify the relationship between the optical properties at the leaf and the canopy scale. This suite of variables and soil reflectance govern the energy conservation in vegetation canopies at any wavelength in the visible and near-infrared portion of the solar spectrum. The objective of this paper is to assess the information content of hyperspectral data with respect to variables that determine optical remote sensing data, and to develop algorithms for retrieving these variables from hyperspectral canopy reflectances.

2. Experimental site, instrumentation, and measurements

A coniferous forest near Ruokolahti, Finland (61.32°N, 28.43°E), was chosen for measurements of canopy transmittances, reflectances, and leaf area index. Field measurements were made between June 14 and 21, 2000. The site is mostly occupied by Scots Pine (*Pinus sylvestris*) and Norway Spruce (*Pices abies*), with pines being dominant. Most of the experimental area was under needle leaf trees with an average height of about 30 m. However, there was a small open area in this 1×1 km site that was occupied by regrowing smaller (less than 1.5 m in height) pine trees and an understory of grasses. The canopy was stratified into young, regular, and dense needle forests based on an airborne 2-m resolution charge-coupled device (CCD) image. A 100×150 m plot was laid out within the dense forest and a grid system was made composed of 25×25 m cells, giving a total 35 grid points. The ground beneath the 100×150 m plot was a dark soil with dead litter of needles.

The hemispherical canopy transmittance (reflectance) for nonisotropic incident radiation is the ratio of the mean downward radiation flux density at the canopy bottom (mean upward radiation flux density at the canopy top) to the downward radiation flux density above the canopy. A LI-1800 spectroradiometer with Standard Cosine Receptor was used to measure spectra of incident radiation flux density in the region from 400 to 1100 nm, at 1-nm resolution. Measurements of spectral downward radiation flux densities, and upward radiation above the 100×150 plot from 350 to 1085 nm, below 1.6 nm were obtained with an ASD hand-held spectroradiometer. These instruments were intercalibrated.

Azimuth-average radiation at five zenith angles were collected with the LAI-2000 Plant Canopy Analyzer composed of a LAI-2070 control unit and a LAI-2050 sensor head. The sensor head projects the image of its nearly hemispheric view onto five detectors arranged in concentric rings (approximately 0–13°, 16–28°, 32–43°, 47–58°, 61–74°). An optical filter in the LAI-2050 sensor rejects radiation above 490 nm. In this blue portion of the solar spectrum, foliage typically reflects and transmits relatively little radiation. LAI-2000 readings, therefore, provide an accurate estimate of uncollided downward radiation field below the vegetation canopy.

The LI-1800 spectroradiometer was placed in an open area to measure the incident radiation. The ASD with a standard cosine receptor was used to collect spectral downward fluxes at each grid point of the 100×150 m plot. To make simultaneous measurements, we used a pair of cell phones for communication. The average of these measurements was taken as the mean downward radiation flux at the bottom of the canopy. The upward radiation field above the canopy was measured by mounting the ASD on a helicopter. The ASD field of view was set to 25° and six measurements were taken at about 30 m above the upper boundary of the 100×150 m plot. The average of these measurements was used to represent spectral variation in the dense forest reflectance. The above- and below-canopy measurements were performed at the same time (14:00, June 20 and 21, 2000) of two consecutive days under clear-sky conditions with few clouds. The solar polar angle at this time was about 43°.

LAI-2000 measurements were made shortly before sunset when the forest was illuminated by diffuse light. Two

LAI-2000 units were used to take simultaneous measurements within the forest and in an open area. They were calibrated to one another. We followed the measurement methodology described in the LAI-2000 plant canopy analyzer instruction manual, Chapter 4-1 (Li-COR, 1992). Mean LAI derived from these measurements was 1.95.

To calibrate the ASD and LI-1800 spectroradiometers, a series of simultaneous measurements of downward radiation fluxes in an open area under various illumination conditions were made. Then, coefficients, $k(\lambda)$, which convert DN values provided by the ASD spectroradiometer to radiometric units (provided by the LI-1800) as a function of different illumination conditions were evaluated as $k(\lambda) = \mathrm{LI}_0(\lambda)/\mathrm{ASD}_0(\lambda)$. Here $\mathrm{LI}_0(\lambda)$ and $\mathrm{ASD}_0(\lambda)$ are calibration measurements taken by the LI-1800 and ASD spectroradiometers, respectively. The coefficients were used to evaluate hemispherical canopy spectral transmittances, $t(\lambda)$, defined as the ratio of the downward radiation flux density at the bottom of the canopy to the downward radiation flux density above the canopy, namely,

$$t(\lambda) = k(\lambda)\frac{\mathrm{ASD}^{\downarrow}(\lambda)}{\mathrm{LI}^{\downarrow}(\lambda)}, \tag{1}$$

where $\mathrm{LI}^{\downarrow}(\lambda)$ and $\mathrm{ASD}^{\downarrow}(\lambda)$ are downward radiation fluxes taken simultaneously by the LI-1800 and ASD spectroradiometers in an open area and below the canopy, respectively.

The hemispherical-directional reflectance factor (HDRF) for nonisotropic incident radiation is the ratio of the mean radiance leaving the top of the plant canopy to radiance reflected from an ideal Lambertian target into the same beam geometry and illuminated under identical atmospheric conditions (Martonchik et al., 1998). The HDRF in the zenith direction was approximated by its mean over the 25° field of view,

$$\begin{aligned}\mathrm{HDRF}(\lambda) &= k'(\lambda)\frac{\mathrm{ASD}^{\uparrow}_{25}(\lambda)}{\pi(1-\mu_0^2)} : \frac{\mathrm{LI}^{\downarrow}(\lambda)}{\pi} \\ &= \frac{k'(\lambda)}{(1-\mu_0^2)}\frac{\mathrm{ASD}^{\uparrow}_{25}(\lambda)}{\mathrm{LI}^{\downarrow}(\lambda)}.\end{aligned} \tag{2}$$

Here $\mu_0 = \cos(12.5°)$, $\mathrm{ASD}^{\uparrow}_{25}(\lambda)$ is the upward radiation field at 30 m above the upper canopy boundary collected by the ASD with 25° field of view, and $\mathrm{LI}^{\downarrow}(\lambda)$ is the downward radiation flux density measured by the LI-1800 in the open area. The calibration coefficient, $k'(\lambda)$, was evaluated from $k'(\lambda)\,\mathrm{ASD}^{\uparrow}_{\mathrm{w},25}(\lambda) = \pi^{-1}\,\mathrm{LI}^{\downarrow}_{\mathrm{w}}(\lambda)\,(1-\mu_0^2)\pi$, where $\mathrm{ASD}^{\uparrow}_{\mathrm{w},25}(\lambda)$ is the radiation reflected by a white Lambertian surface and registered by the ASD with 25° field of view, and $\mathrm{LI}_0(\lambda)$ is the downward radiation flux density incident on the white Lambertian surface and registered by the LI-1800. Measurements of the radiation incident and reflected by the white surface were taken simultaneously. The measured HDRFs were taken as the hemispherical canopy reflectance $r(\lambda)$ defined as the ratio between upward and downward radiation flux densities above the vegetation canopy.

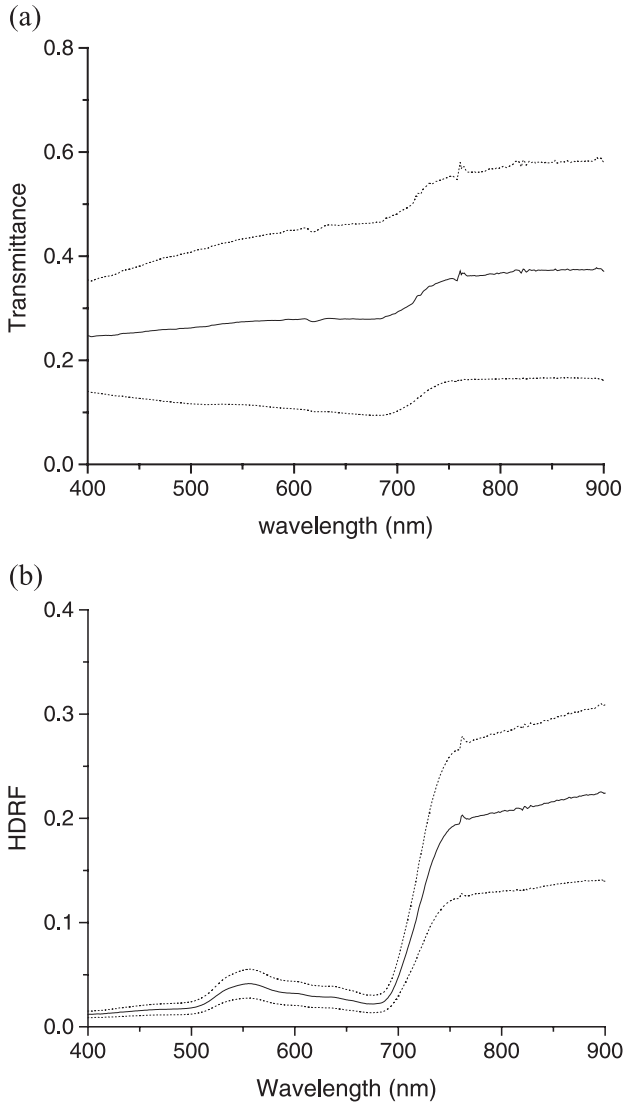

Fig. 1. (a) Spectral variation (solid line) of mean hemispherical canopy transmittance and (b) mean hemispherical–directional reflectance factor (solid line) derived from data collected at the 100 × 150 m area. Dotted curves denote ± 1 S.D.

Fig. 1 demonstrates the mean spectral HDRF and transmittance, and their standard deviations. These curves were used in all calculations presented in this paper. Heterogeneity of the canopy caused large uncertainties in these spectra.

3. Radiative transfer in vegetation canopies: theory

3.1. The law of energy conservation

The linear transport equation is used to describe radiative transfer process in the vegetation canopy (Myneni, 1991; Ross, 1981; Zhang, Shabanov, Knyazikhin, & Myneni, 2002; Zhang, Tian, Myneni, Knyazikhin, & Woodcock, 2002). This equation has a simple physical interpretation;

it is a mathematical statement of the energy conservation law. The forest is idealized as a horizontally homogeneous medium bounded at the bottom by a Lambertian surface. An impact of this idealization on the description of the radiative transfer process will be discussed in Section 5. Under this assumption, the solution, $I_\lambda(z,\Omega)$, to the transport equation can be written as (Box, Gerstl, & Simmer, 1988; Chandrasekhar, 1950, p. 273; Stamnes, 1982; van de Hulst, 1981, p. 64)

$$I_\lambda(z,\Omega) = I_{BS,\lambda}(z,\Omega) + \frac{\rho_\lambda}{1-\rho_\lambda r_{S,\lambda}} F_{BS,\lambda} I_{S,\lambda}(z,\Omega). \quad (3)$$

Here $I_\lambda(z,\Omega)$ is the monochromatic intensity, which depends on wavelength λ, depth z below the upper canopy boundary, and direction Ω. The first term, $I_{BS,\lambda}(z,\Omega)$ is the intensity of radiation field in the same vegetation canopy, but bounded at the bottom by a nonreflecting surface (the "black soil" problem). The second term describes the additional radiative field due to interactions between the underlying surface and the vegetation canopy (named as "S" problem), and includes the following components: the hemispherical reflectance, ρ_λ, of the underlying surface; the downward flux density, $F_{BS,\lambda}$, at the bottom of the canopy for the black soil problem; intensity, $I_{S,\lambda}$, of the radiation field in the same canopy illuminated from the bottom by a normalized isotropic source $Q_S = 1/\pi$ (in sr^{-1}); and $r_{S\lambda}$ is the downward flux density at the surface generated by Q_S. This decomposition of the radiation field allows the separation of three independent variables responsible for the distribution of solar radiation in vegetation canopies; that is, the reflectance ρ_λ of the underlying surface that does not depend on the vegetation canopy; $I_{BS,\lambda}$ and $I_{S,\lambda}$, which are surface-independent parameters since no multiple interactions between the medium and the underlying surface are possible, i.e., these variables have intrinsic canopy information.

Let $r(\lambda)$, $t(\lambda)$, and $a(\lambda)$ be the canopy transmittance, reflectance, and absorptance. Here the canopy absorptance is defined as the ratio of energy absorbed by vegetation to the total incident irradiance. It follows from Eq. (3) that these variables can be expressed as

$$r(\lambda) = r_{BS}(\lambda) + \frac{\rho_\lambda}{1-\rho_\lambda r_S(\lambda)} t_{BS}(\lambda) t_S(\lambda), \quad (4)$$

$$t(\lambda) = t_{BS}(\lambda) + \frac{\rho_\lambda}{1-\rho_\lambda r_S(\lambda)} t_{BS}(\lambda) r_S(\lambda) = \frac{t_{BS}(\lambda)}{1-\rho_\lambda r_S(\lambda)}, \quad (5)$$

$$a(\lambda) = a_{BS}(\lambda) + \frac{\rho_\lambda}{1-\rho_\lambda r_S(\lambda)} t_{BS}(\lambda) a_S(\lambda). \quad (6)$$

Here r_{BS} and r_S; t_{BS} and t_S; a_{BS} and a_S are the canopy reflectance, transmittance, and absorptance for the "black soil" (subscript "BS") and "S" (subscript "S") problems, respectively. These variables depend on canopy structure and optical properties of individual leaves. They are related via the energy conservation law

$$r_{BS} + t_{BS} + a_{BS} = 1, \quad r_s + t_s + a_s = 1. \quad (7)$$

The magnitude of scattering per element foliage volume is described using single-scattering albedo, $\omega(\lambda)$, which is defined as the ratio of energy scattered by the elementary volume to energy intercepted by this volume. This variable is assumed constant with respect to spatial and directional variables in our study. However, the single-scattering albedo depends on the definition of the scattering center and the size of the elementary volume. For example, if a cube of $50 \times 50 \times 50$ cm is taken as an elementary volume in a coniferous forest, a 1-year shoot of 5–7 cm should be taken as a scattering center (Knyazikhin, Mieben, Panfyorov, & Gravenhorst, 1997). The single-scattering albedo, in this case, characterizes scattering properties of the $50 \times 50 \times 50$ cm cube filled with 1-year shoots, and all coefficients of the transport equation should be derived for such $50 \times 50 \times 50$ cells. Thus, the scattering center and the size of the elementary volume must be consistent in order to correctly evaluate the canopy radiation regime with the radiative transfer equation (Tian et al., in press). The following criteria can be applied to achieve this consistency: the elementary volume is a volume inside which photon can undergo not more than one interaction with scattering centers (Van de Hulst, 1981, p. 5). In our study, 1-year shoots of 5–7 cm are taken as the scattering centers, and the elementary volume is assumed to be a $50 \times 50 \times 50$ cm cube. Such a specification of scattering centers and elementary volume allows the transport equation to predict the radiative regime in a coniferous forest of about 40×40 m within an uncertainty of about 20% (Knyazikhin et al., 1997).

3.2. Canopy spectral invariance

Our next step is to separate the single-scattering albedo from canopy transmittances and absorptances. Let $i_v(\lambda)$ be the canopy interception, defined as the canopy absorptance $a_v(\lambda)$ normalized by the absorptance $1-\omega(\lambda)$ of the elementary volume, i.e.,

$$i_v(\lambda) = \frac{a_v(\lambda)}{1-\omega(\lambda)} = \frac{1-t_v(\lambda)-r_v(\lambda)}{1-\omega(\lambda)}. \quad (8)$$

Here and throughout the text, the symbol v indicates either the "black soil" (v = "BS") or "S" (v = "S") problems. For a vegetation canopy bounded at its bottom by a black surface, this variable is the mean number of photon interactions with leaves at wavelength λ before either being absorbed or exiting the canopy. We term this variable canopy interception. The canopy spectral invari-

ance for canopy interception states that the variable $p_{i,v}$ defined as

$$p_{i,v} = \frac{i_v(\lambda_0) - i_v(\lambda_1)}{\omega(\lambda_0) i_v(\lambda_0) - \omega(\lambda_1) i_v(\lambda_1)}, \quad (9)$$

remains constant for any arbitrary chosen wavelengths λ_0 and λ_1 (Knyazikhin et al., 1998; Panferov et al., 2001; Shabanov et al., in preparation).

The spectral canopy transmittance possesses a similar property. However, the variable

$$p_{t,v} = \frac{t_v(\lambda_0) - t_v(\lambda_1)}{\omega(\lambda_0) t_v(\lambda_0) - \omega(\lambda_1) t_v(\lambda_1)}, \quad (9a)$$

can take on several values depending on whether the canopy transmittance is a multi- or single-value function with respect to the single-scattering albedo. Fig. 2 illustrates this criterion. One can note that the canopy transmittance can be a multi-value function with respect to the single-scattering albedo. Three single-value functions corresponding to three wavelength intervals, namely, $487 \le \lambda < 555$ nm, $555 \le \lambda < 650$ nm, and $650 \le \lambda \le 900$ nm, can be separated from this curve. Within each spectral interval, the variable $p_{t,BS}$ is insensitive to couples (λ_0, λ_1). In this particular case, $p_{t,BS}$ takes on three interval specific values, namely, 0.10, 0.85, and 0.48 (Panferov et al., 2001). It should be noted that the canopy transmittance in the interval $400 \le \lambda < 487$ nm can vary considerably, with the single-scattering albedo essentially unchanged. The canopy structure variable $p_{t,BS}$ cannot be specified in this case (see Panferov et al., 2001). It should be emphasized that $p_{t,BS}$ does not depend on the single-scattering albedo. However, this variable can be sensitive to the portion f_{dir} of direct solar beam in the total radiation incident on the canopy (Section 3.3).

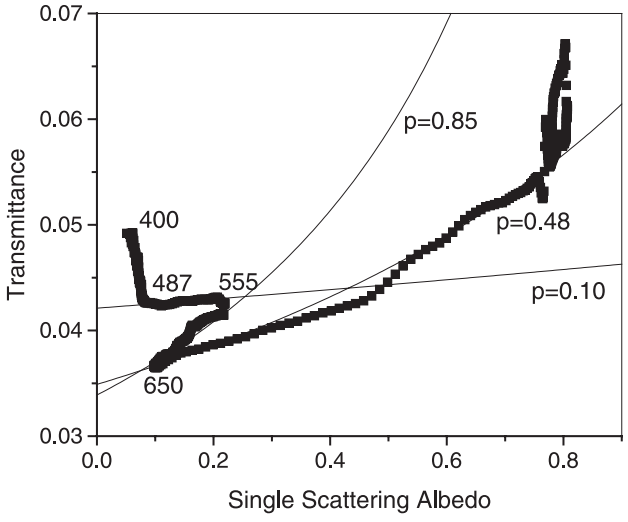

Fig. 2. Canopy hemispherical transmittance as a function of the single-scattering albedo (dotted line) for the Solling site, Goettingen, Germany (from Panferov et al., 2001). Three single-value curves [$t(\lambda)$, $\omega(\lambda)$] corresponding to three intervals $487 \le \lambda < 555$, $555 \le \lambda < 650$, and $\lambda \ge 650$ nm, can accurately be approximated with Eq. (10) using $p_{t,BS} = 0.10$, 0.85, and 0.48, respectively (solid lines). It means that the spectral invariance (Eq. (9a)) takes place for each of these intervals. In this example, the canopy transmittance corresponding to the interval $400 \le \lambda < 487$ nm can vary considerably with the single-scattering albedo essentially unchanged.

The canopy spectral invariance results in a relation between canopy transmittance, $t_v(\lambda_0)$, and interception, $i_v(\lambda_0)$, at an arbitrary chosen reference wavelength λ_0 to transmittances, $t_v(\lambda)$, and interceptions, $i_v(\lambda)$, at all other wavelengths,

$$t_v(\lambda) = \frac{1 - p_{t,v}\omega(\lambda_0)}{1 - p_{t,v}\omega(\lambda)} t_v(\lambda_0),$$
$$i_v(\lambda) = \frac{1 - p_{i,v}\omega(\lambda_0)}{1 - p_{i,v}\omega(\lambda)} i_v(\lambda_0), \quad v = \text{“BS”, “S”}. \quad (10)$$

The canopy spectral invariants are formulated in terms of the single-scattering albedo $\omega(\lambda)$. The left-hand side of Eq. (10) can be directly derived from field measurements irrespective of the definition of the single-scattering albedo. It means that the coefficients p_t and p_i depend on the scale at which the single-scattering albedo is introduced. We have two variables to characterize “the leaf scale,” namely, the single-scattering albedo and the coefficients $p_{t,v}$ and $p_{i,v}$. Thus, Eq. (10) specify relationships between the optical properties at the leaf and the canopy scales. It should be noted that the products $p_{t,v}\omega(\lambda)$ and $p_{i,v}\omega(\lambda)$ became scale-independent variables.

There are several interpretations of the parameters $p_{t,v}$ and $p_{i,v}$ reported in literature. First, $p_{t,v}\omega(\lambda)$ and $p_{i,v}\omega(\lambda)$ are the maximum positive eigenvalues of linear operators describing canopy transmittance and radiation field in the vegetation canopies (Knyazikhin et al., 1998; Zhang, Shabanov, et al., 2002; Zhang, Tian, et al., 2002). Panferov et al. (2001) found that $p_{i,v} = 1 - N_1/N_2$, where N_1 and N_2 are counts of photon interactions with absorbing ($\omega = 0$) and scattering ($\omega = 1$) leaves, respectively (interpretation of the parameter $p_{t,v}$ can be found in Panferov et al., 2001). Shabanov et al. (in preparation) treated these variables as follows. For a purely absorbing medium, i.e., $\omega = 0$, transmittance q_t is the probability that a photon in the incident radiation will arrive at the bottom of the canopy without suffering a collision (uncollided radiation), while the interception $q_i = 1 - q_t$ coincides with the probability of its absorption. Substituting $\omega(\lambda_0) = 0$, q_t and q_i into Eq. (10), one obtains

$$t_v(\lambda) = \frac{1}{1 - p_{t,v}\omega(\lambda)} q_t, \; i_v(\lambda) = \frac{1}{1 - p_{i,v}\omega(\lambda)} (1 - q_t). \quad (10a)$$

Solving these equation for $p_{t,v}\omega(\lambda)$ yields $p_{t,v}\omega(\lambda) = [t_v(\lambda) - q_t]/t_v(\lambda)$ and $p_{i,v}\omega(\lambda) = [i_v(\lambda) - q_i]/i_v(\lambda)$. Thus, $p_{t,v}\omega(\lambda)$ and $p_{i,v}\omega(\lambda)$ are portions of collided radiation in total radiation transmitted and intercepted by the vegetation canopy, respectively. This interpretation will be used in further discussions here.

3.3. Parameterization of the short-wave energy balance in the 100×150 m plot

The ground at the experimental plot is a dark soil. Therefore, we neglect its contribution to the radiation regime of the canopy by assuming reflectance $\rho\lambda$ equal to zero. In this case, the short-wave energy balance can be parameterized in terms of t_{BS} and a_{BS}, which, in turn, are functions of the single-scattering albedo $\omega(\lambda)$, two canopy structure-specific variables, $p_{t,BS}$ and $p_{i,BS}$, and the uncollided radiation fraction q_t. The canopy reflectance $r_{BS}(\lambda)$ can be specified via the energy conservation law (Eq. (7)). All these variables (except $p_{i,BS}$, Knyazikhin et al., 1998) depend on the direction, Ω_0, of solar radiation incident on the canopy. This parameter suite is primarily responsible for the generation of optical remote sensing data, which, in turn, can be related to other biophysical variables characterizing the vegetated surface. This is demonstrated with the following examples.

The ground cover is an important characteristic of the canopy structure, which is the fraction of ground covered by crowns projected vertically. It can be evaluated as $1-q_n$, where q_n is the probability that a photon entering the vegetation canopy along the nadir direction Ω_n will arrive at the bottom of the canopy through gaps in the stand. In the classical radiative transfer theory, the uncollided radiation $q_{t,dir}(\Omega_0)$ in the direction Ω_0 is given by the Beer's law (Ross, 1981),

$$q_{t,dir}(\Omega_0) = \exp\left(-\mathrm{LAI}\frac{G(\Omega_0)}{|\mu_0|}\right). \quad (11)$$

Here LAI is the leaf area index, $G(\Omega_0)$ is the mean projection of leaf normals in the direction Ω_0, and μ_0 is the cosine of polar angle of the direction Ω_0. In terms of this notation, q_n coincides with q_t in the nadir direction Ω_n, i.e., $q_n = q_t(\Omega_n)$. Given $q_{t,dir}(\Omega_0)$ in the direction of the direct solar beam, the ground cover can be expressed as

$$\begin{aligned} 1-q_n &= \exp(-\mathrm{LAI}\cdot G(\Omega_n)) \\ &= 1-\exp\left(-\mathrm{LAI}\frac{G(\Omega_0)}{|\mu_0|}\frac{|\mu_0|G(\Omega_n)}{G(\Omega_0)}\right) \\ &= 1-q_{t,dir}(\Omega_0)^{|\mu_0|\frac{G(\Omega_n)}{G(\Omega_0)}}. \end{aligned} \quad (12)$$

If the vegetation canopy is illuminated by a diffuse radiation field, the portion $q_{t,diff}$ of uncollided radiation takes the form:

$$q_{t,diff} = \int_0^1 d\mu \int_0^{2\pi} d\varphi |\mu| \exp\left(-\mathrm{LAI}\frac{G(\Omega)}{|\mu|}\right). \quad (13)$$

Thus, the probability q_t that a photon in the incident radiation will arrive at the bottom of the canopy without suffering a collision depends on the direction Ω_0 of the solar beam and the portion f_{dir} of direct radiation in the total radiation incident on the canopy. This parameter can be approximated as

$$q_t = f_{dir}q_t(\Omega_0) + (1-f_{dir})q_{t,diff}. \quad (14)$$

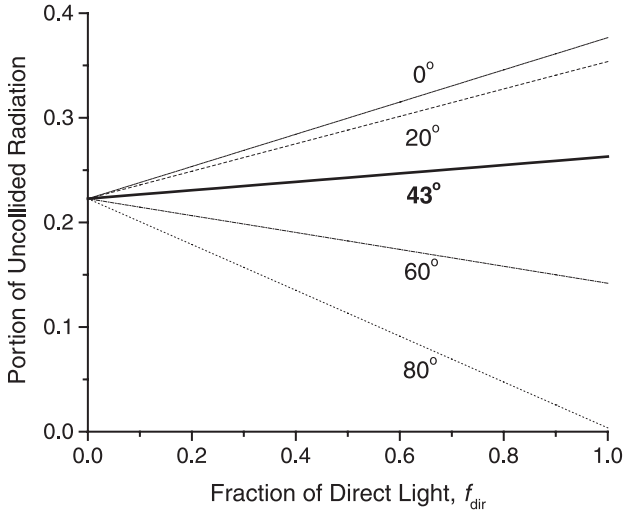

Fig. 3. The portion q_t of uncollided radiation as a function of the fraction f_{dir} of the direct solar beam for different solar zenith angles. These curves are described by Eq. (14). The leaf area index is 2 and leaves are assumed uniformly distributed ($G_0 = 0.5$).

Fig. 3 shows q_t as a function of f_{dir} for different values of the solar zenith angle.

The probability q_t derived from hyperspectral data can be used to solve Eq. (11) for the leaf area index. Also, $p_{t,BS}$ and $p_{i,BS}$ are determined by the canopy structure, which does not depend on wavelength. Hyperspectral data therefore convey considerable information about the structural properties of vegetation canopies. The single-scattering albedo, $\omega(\lambda)$, is related to chemical and biophysical processes in leaves (Blackburn, 1998; Zarco-Tejada, Miller, Mohammed, & Noland, 2000). Knowing $\omega(\lambda)$, $p_{t,BS}$, and $p_{i,BS}$, for example, one can relate the spectral behavior of the entire canopy to the biophysical, chemical, and physical processes at the leaf scale. The suite of these basic canopy parameters provides a powerful tool for monitoring the functioning of plants.

4. Information content of hyperspectral data

For any arbitrary chosen wavelengths λ_1, λ_2, and λ_3 ($\lambda_i \neq \lambda_j$, $i, j = 1,2,3$), the following system of nine equations can be composed from (Eqs. (7), (8), and (10a),

$$r_{BS}(\lambda_k) + t_{BS}(\lambda_k) + a_{BS}(\lambda_k) = 1, \quad k = 1,2,3; \quad (15a)$$

$$t_{BS}(\lambda_k) = \frac{1}{1-p_{t,BS}\omega(\lambda_k)}q_t, \quad k = 1,2,3; \quad (15b)$$

$$\frac{a_{BS}(\lambda_k)}{1-\omega(\lambda_k)} = \frac{1}{1-p_{i,BS}\omega(\lambda_k)}(1-q_t), \quad k = 1,2,3. \quad (15c)$$

Note that Eqs. (15a)–(15c) each includes three equations corresponding to three different values of λ. This system relates 15 variables. They are canopy absorptance, trans-

Table 1
Correspondence between given variables and variables retrievable from this information

Known variables	Unknown variables
$t(\lambda)$, $r(\lambda)$	$\omega(\lambda)$, $p_{i,BS}$, $p_{t,BS}$, q_t, $a(\lambda)$
$r(\lambda)$, $\omega(\lambda)$	$t(\lambda)$, $p_{i,BS}$, $p_{t,BS}$, q_t, $a(\lambda)$
$r(\lambda)$, q_t, $p_{i,BS}$, $p_{t,BS}$	$\omega(\lambda)$, $t(\lambda)$, $a(\lambda)$
$\omega(\lambda)$, $p_{i,BS}$, $p_{t,BS}$, q_t	$r(\lambda)$, $t(\lambda)$, $a(\lambda)$

mittance, reflectance, and the single-scattering albedo at three wavelengths, λ_1, λ_2, and λ_3; and three canopy structure-specific variables, q_t, $p_{t,BS}$, and $p_{i,BS}$. Given values of six arbitrary chosen variables, one can solve this system for the rest of nine variables. By formulating this system for all possible combinations of wavelengths, one obtains an infinite system of equations that relates seven variables, namely, four spectral (transmittance, reflectance, absorptance, and the single-scattering albedo) and three canopy structure specific parameters (q_t, $p_{t,BS}$, and $p_{i,BS}$). Given a part of them, the rest can be specified from the infinite system of equations. Table 1 shows correspondences between given variables and retrieved variables. One can see that information on any two spectra is sufficient to retrieve the reminder set of canopy parameters. One can also see that the three canopy structure specific parameters, q_t, $p_{t,BS}$, and $p_{i,BS}$, convey the same amount of information as one spectrum.

We focus on finding the spectra of the single-scattering albedo $\omega(\lambda)$ and three canopy structure specific variables, q_t, $p_{t,BS}$, and $p_{i,BS}$, from canopy spectral reflectances $r_{BS}(\lambda)$ and transmittances $t_{BS}(\lambda)$. The canopy spectral absorptance $a_{BS}(\lambda)$ at any wavelength can be obtained from Eq. (15a). The following algorithm is applied to find the rest of parameters. Given λ_1, λ_2, and λ_3, we solve the equation system (Eqs. (15a)–(15c)) for the single-scattering albedo (λ_k, ω_k) at three wavelengths ($k=1, 2, 3$), and three canopy structure specific parameters. Repeating this process for all possible combination of λ_1, λ_2, and λ_3, one obtains four sets of solutions (Appendix A). To specify the canopy structure specific parameters, one derives histograms of q_t, $p_{t,BS}$, and $p_{i,BS}$, and then takes their most probable values as the desired solutions. The distribution of single-scattering albedo values is given by a bivariate distribution function defined as number of solutions (λ, ω) per unit area in the λ–ω plane. The most probable value of ω corresponding to the wavelength λ is taken as the retrieved single-scattering albedo at this wavelength.

5. Results

Canopy spectral transmittances and reflectances collected during the field campaign were used to derive the suite of canopy parameters. The spectral interval [400, 900 nm] was divided into four subintervals, 400–487 nm, 487–555 nm, 555–650 nm, 650–900 nm, and the algorithm described in the previous section and Appendix A was applied to each of these intervals. The portion f_{dir} of direct solar beam is assumed constant within each interval.

Fig. 4 shows histograms of q_t. In all cases, the most probable value of q_t can be specified from the infinite system of equations sufficiently well (see Table 2). Given

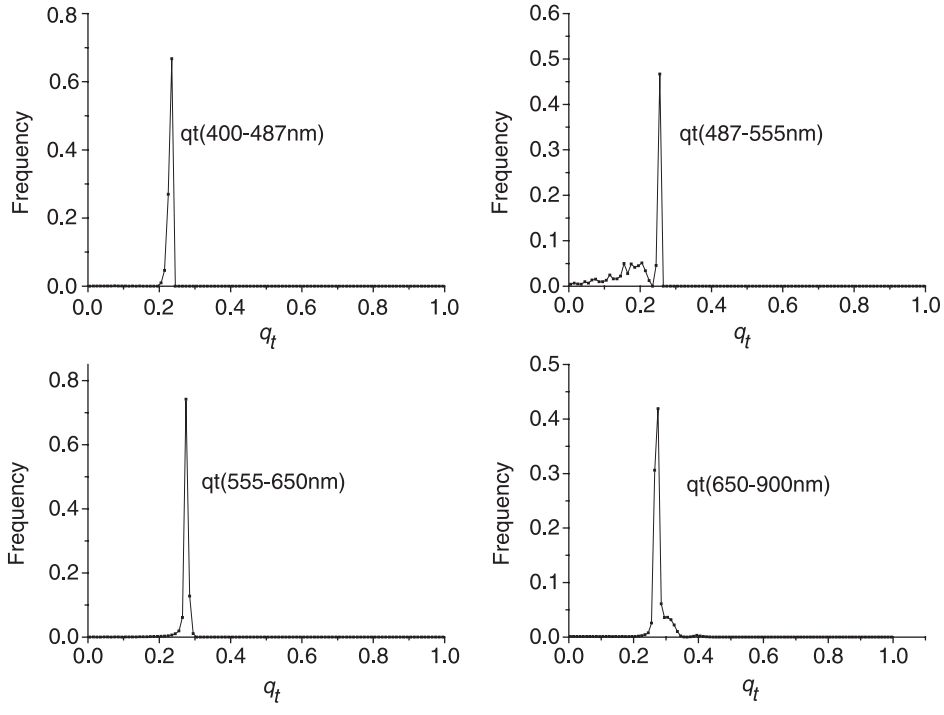

Fig. 4. Histogram of q_t at four spectral intervals.

Table 2
Retrieved values of q_t and $p_{t,BS}$

Retrieved parameters	400–487 nm	487–555 nm	555–650 nm	650–900 nm
q_t	0.235	0.255	0.275	0.275
$p_{t,BS}$	–	0.3	0.05	0.45

the direction Ω_0 of the solar beam, the parameter q_t is a function of the portion f_{dir} of the direct solar beam in the total radiation incident on the canopy (Fig. 3), which, in turn, is a wavelength-dependent variable. The solar radiation is more affected by the atmosphere at lower wavelengths. The fraction f_{dir} is therefore an increasing function with respect to the wavelength. Because q_t varies linearly with f_{dir} (Eq. (14) and Fig. 3), the parameter q_t is an increasing function with respect to the wavelength. Retrievals follow this regularity; that is, values of q_t corresponding to spectral subintervals 400–487, 487–555, and 555–900 nm form an increasing sequence of numbers: 0.24, 0.26, and 0.28 (Table 2). The mean value of q_t over all solutions and its standard deviation are 0.25 and 0.06, respectively. Assuming uniform distribution of leaf normals ($G=0.5$), the ground cover evaluated with Eq. (12) is 0.64. Neglecting the diffuse component of the incident radiation (i.e., putting $f_{dir}=1$) and solving Eq. (11) for LAI, one obtains LAI = 2.02. This LAI value is similar to that derived from data collected with the LAI-2000 Plant Canopy Analyzer (LAI = 1.95). Next, solving Eq. (14) using the retrieved LAI and retrieved values of q_t, one can obtain four values, 0.45, 0.60, 0.95, and 0.95, of the ratio f_{dir} corresponding to the spectral intervals specified earlier. Thus, about 55%, 40%, 5%, and 5% of solar radiation in these spectral intervals was scattered by the atmosphere.

We treat solutions (λ, ω) of the infinite system of Eqs. (15a)–(15c) as realizations of a random vector (η_λ, η_ω). Its distribution in the λ–ω plane is given by a bivariate function. To approximate this function, we partition the λ–ω plane into small rectangular boxes and count how many solutions (λ, ω) of the infinite system (Eqs. (15a)–(15c)) fall in each box. Fig. 5a shows these counts. One can see that the most probable realizations of the random vector (η_λ, η_ω) form a curve. A regression curve $\omega(\lambda)=E(\eta_\omega|\eta_\lambda=\lambda)$ of η_ω with respect to the wavelength and its standard deviation are taken as the desired single-scattering albedo and its uncertainty. Here $E(\eta_\omega|\eta_\lambda=\lambda)$ is expectation of the random variable η_ω under the condition that the random variable η_λ has taken the value λ. The regression curve $\omega(\lambda)$ is the best possible prediction of η_ω given a realized value of η_λ (Bronshtein & Semendyayev, 1985, p. 616). Fig. 5b shows the retrieved spectrum of the single-scattering albedo. One can see that the retrieved spectrum has the basic scattering features of a green leaf; that is, local minimum at blue and red wavelengths, local maximum at green, and a sharp jump at $\lambda=700$ nm. Note that the retrieval uncertainties are comparable to uncertainties in input data (see Fig. 1).

Fig. 6 shows histograms of $p_{t,BS}$, which localize three values (Table 2) corresponding to intervals $487 \le \lambda < 555$, $555 \le \lambda < 650$, and $650 \le \lambda < 900$ nm, respectively. However, the algorithm has not localized this parameter for the interval $400 \le \lambda < 487$. The canopy transmittance in this interval can considerably vary with the single-scattering albedo essentially unchanged (Fig. 2), and thus Eq. (15b) does not provide a reliable relationship between canopy transmittance and $p_{t,BS}$. An accurate analysis of this case is given in Panferov et al. (2001).

The histogram of $p_{i,BS}$ is shown in Fig. 7. The most probable value of $p_{i,BS}$ is 0.62. It should be emphasized that $p_{i,BS}$ depends on neither leaf optical properties nor incident radiation, i.e., it is a canopy structure specific variable (Knyazikhin et al., 1998). However, unlike other parame-

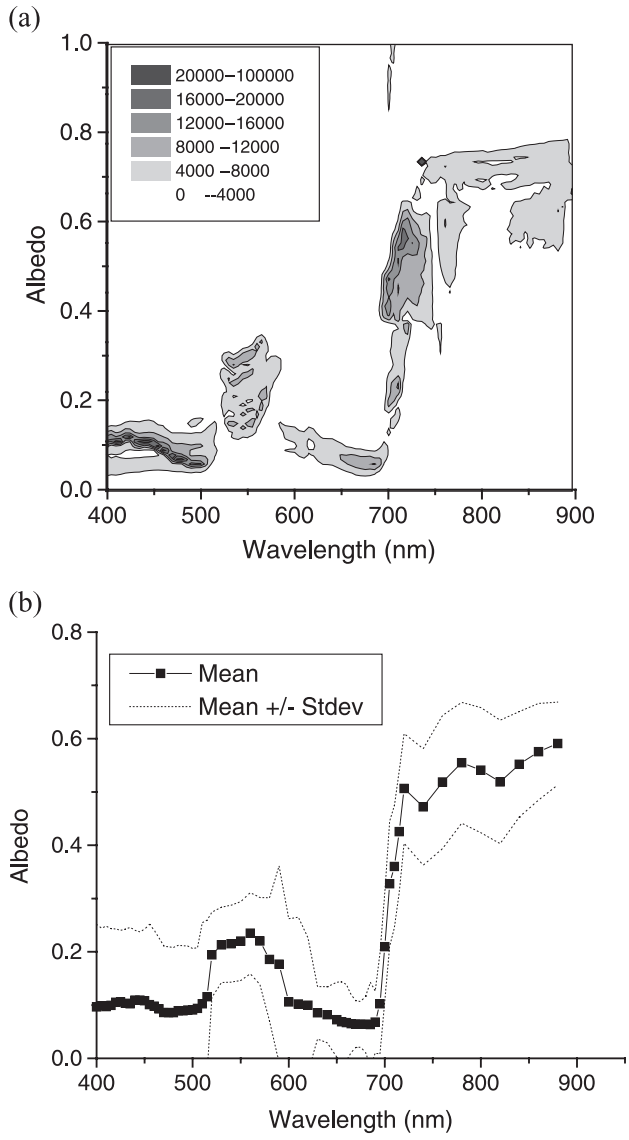

Fig. 5. (a) Bivariate distribution function for the solutions (λ, ω) to the infinite system (Eqs. (15a)–(15c)); (b) Regression curve $\omega(\lambda)$ and its standard deviation derived from the bivariate distribution are taken as the desired single-scattering albedo and its uncertainty.

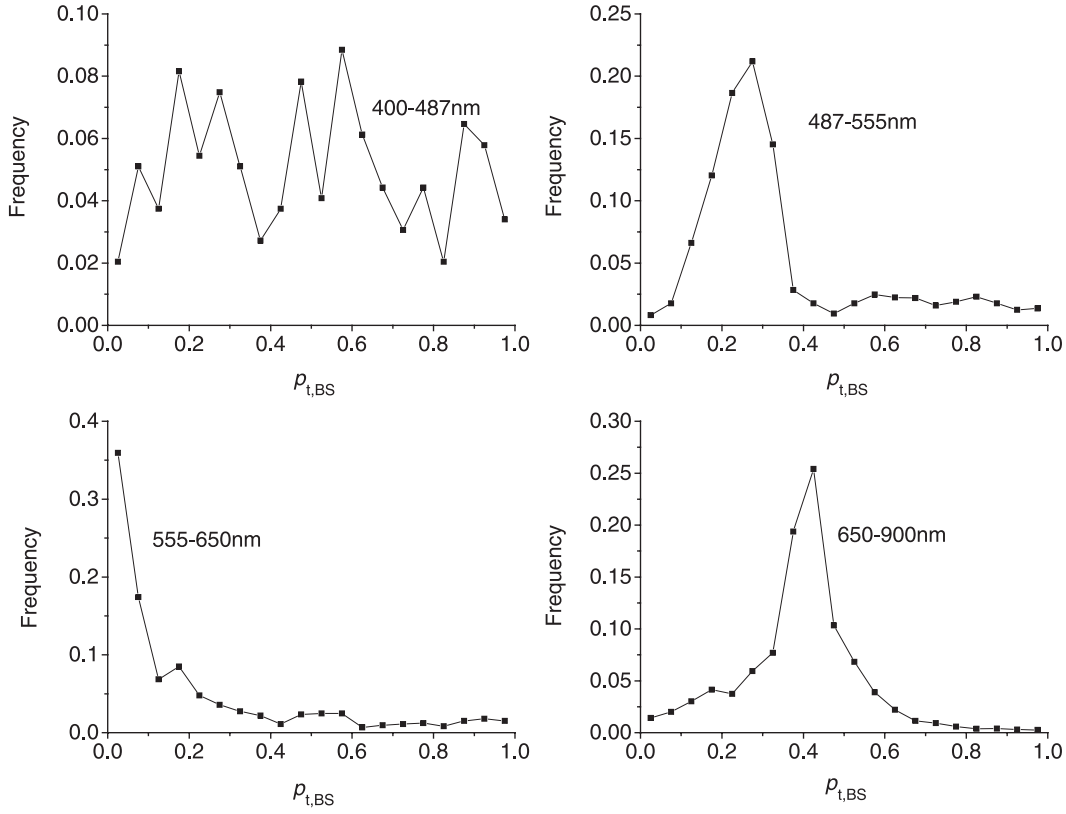

Fig. 6. Histograms of retrieved $p_{t,BS}$ corresponding to four spectral intervals.

ters, information on both canopy spectral reflectance and transmittance is required to specify $p_{i,BS}$ (see Eq. (15c)). Therefore, uncertainties in these input variables as well as uncertainties due to the neglect of surface reflection properties render the histogram wider, and the probability of spectral invariance (Eq. (9)) is consequently reduced.

Given q_t, $p_{t,BS}$, $p_{i,BS}$, and a spectrum of the single-scattering albedo, the spectra of three basic components of the energy conservation law (transmittance, reflectance, and absorptance) for the "black soil" problem can be calculated using (Eqs. (7), (8) and (10a). Figs. 8 and 9 demonstrate the correlation between measured and calculated canopy spectral transmittance and absorptance. The calculated and measured values agree sufficiently well, except in situations where the contribution of the canopy ground to the radiation regime cannot be neglected ($720 \le \lambda < 900$). In this case, the

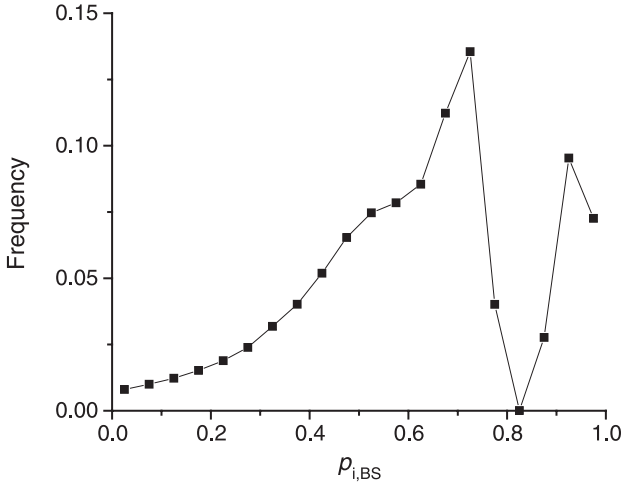

Fig. 7. Histogram of $p_{i,BS}$ corresponding to the spectral interval $400 \le \lambda \le 900$ nm.

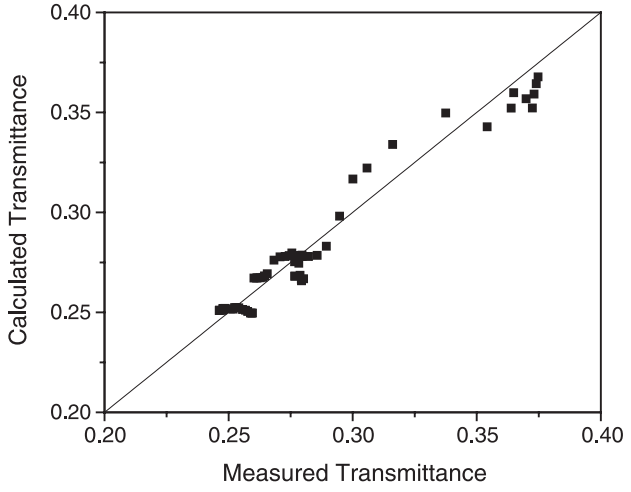

Fig. 8. Measured and calculated canopy transmittances. Calculated canopy transmittance refers to the "black soil" problem.

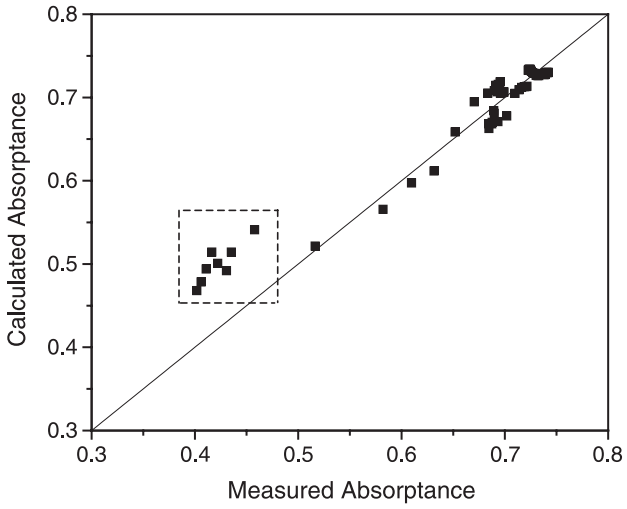

Fig. 9. Measured and calculated canopy absorptance. Calculated canopy absorptance refers to the "black soil" problem. The square separates values of measured and calculated absorptance in the spectral interval $720 \le \lambda \le 900$.

canopy absorptance $a(\lambda) = 1 - t(\lambda) - r(\lambda)$ derived from field data underestimates values of $a_{BS}(\lambda)$. Indeed, it follows from Eqs. (4)–(6) that

$$a(\lambda) = 1 - r(\lambda) - t(\lambda) = a_{BS}(\lambda) - \frac{\rho_\lambda}{1 - \rho_\lambda r_S(\lambda)}(t_S(\lambda) + r_S(\lambda)) \le a_{BS}(\lambda).$$

This inequality for $720 \le \lambda < 900$ nm is clearly seen in Fig. 9. This indicates that the infinite system (Eqs. (15a)–(15c)) allows the removal of the effect of soil reflectance from measured canopy spectral transmittance and absorptance, and specify variables $a_{BS}(\lambda)$ and $t_{BS}(\lambda)$, which have intrinsic canopy information.

6. Sources of uncertainties

The canopy is idealized as a horizontally homogeneous medium bounded at the bottom by a Lambertian surface. This assumption allows the specification of a complicated radiative transfer problem as two independent, simpler subproblems ("black soil" problem and "S" problem). Somewhat more complicated techniques have been developed to do the same in the case of the three-dimensional radiative transfer equation (Bell & Glasstone, 1970; Ioltukhovski, 1999; Knyazikhin & Marshak, 2000; Knyazikhin et al., 1998). Although the second term in Eq. (3) describing radiation field due to the interactions between the underlying surface and the vegetation canopy cannot be expressed in such a simple form in the three-dimensional case, its physical meaning remains unchanged; that is, three-dimensional radiation field can be expressed in terms of ground reflectance properties; the radiation field in the medium bounded at the bottom by a black surface; and the radiation field in the medium generated by anisotropic heterogeneous wavelength-independent sources located at the surface underneath the medium. The ground at the experimental plot is a dark soil. The contribution of the underlying surface to the canopy radiation regime, therefore, was neglected; i.e., only the first component in Eq. (3) was used to describe photon–canopy interactions in this study.

The canopy spectral invariants were derived for the "black soil" and "S" problems in the general case of three-dimensional radiation fields (Knyazikhin et al., 1998). Thus, our assumption regarding homogeneity of the vegetation canopy is not essential to analyses presented in this paper.

Measured spectral canopy transmittance $t(\lambda)$ and the transmittance $t_{BS}(\lambda)$ calculated for the black soil problem are related as $t(\lambda) = t_{BS}(\lambda)/(1 - \rho_\lambda r_S(\lambda))$ (cf. Eq. (5)). Neglecting the contribution of the underlying surface has a minimal effect on the determination of q_t and $p_{t,BS}$ if $\rho_\lambda r_S(\lambda)$ varies with λ insignificantly as compared with variation in $t(\lambda)$. This condition is usually satisfied. A method to minimize the impact of the term $\rho_\lambda r_S(\lambda)$ on the specification of q_t and $p_{i,BS}$ is detailed in Shabanov et al. (in preparation). Given q_t and $p_{t,BS}$, the spectral single-scattering albedo is determined by Eq. (15b) and thus uncertainties in $\omega(\lambda)$ are mainly due to uncertainties in the canopy spectral transmittance $t_{BS}(\lambda)$. However, because the single-scattering albedo also satisfies Eq. (15c), uncertainties in canopy reflectance can also influence its accuracy.

Because information on both reflectance and transmittance is required to derive $p_{i,BS}$, uncertainties in these as well as uncertainties due to ignoring the surface contribution can result in a wider histogram of $p_{i,BS}$. These factors decrease the probability of the spectral invariance (Eq. (9)). Because $p_{i,BS}$ depends on neither leaf optical properties nor incident radiation, one should use those wavelengths at which contribution of soil reflectance is minimum, namely, those wavelength at which variation in canopy transmittance significantly larger than variation in soil reflectance (Shabanov et al., in preparation).

Another source of uncertainty in our experiment is the use the HDRF to approximate the hemispherical canopy reflectance. The ASD field of view was 25° and the HDRF derived from field measurements was assumed to represent the hemispherical canopy reflectance.

7. Conclusions

Empirical and theoretical analyses of hyperspectral canopy transmittance and reflectance collected during a field campaign in Roukolahti, Finland, June 14–21, indicate that spectral response of the vegetation canopy to the incident solar radiation can be fully described by a small set of independent variables. They are the soil reflectance, canopy transmittance, reflectance and interception, the single-scat-

tering albedo, the portion uncollided radiation in the total incident radiation, and portions of collided radiation intercepted and transmitted by the vegetation canopy. All of these are measurable; they satisfy a simple system of equations that specify canopy spectral behavior at leaf and canopy scales. An algorithm for solving this system has been developed and implemented to retrieve these parameters given canopy transmittance and reflectance spectra. Results from this study suggest that the information content of hyperspectral data can be fully exploited if these independent variables are first retrieved, for they can be more directly related to biophysical properties of the vegetation canopy. More research and data are needed to verify this hypothesis. However, as it was shown in this paper, the retrieved variables can be used to estimate canopy leaf area index, vegetation ground cover, the ratio of direct to total incident solar radiation at blue, green, red, and near-infrared spectral intervals.

Acknowledgements

This research was carried out jointly by the personnel at Boston University, University of Helsinki, Finnish Forest Research Institute, and VTT Automation, Remote Sensing Group, Finland. Boston University research is performed under contract with the National Aeronautic and Space Administration.

Appendix A. Solution of the system of Eqs. (15a)–(15c)

Given values t_k and a_k of canopy transmittance $t_{BS}(\lambda_k)$ and absorptance $a_{BS}(\lambda_k)=1-t_{BS}(\lambda_k)-r_{BS}(\lambda_k)$ at three arbitrarily chosen different wavelengths λ_k, $k=1, 2, 3$, we solve Eqs. (15b) and (15c) for values of the single-scattering albedo at three wavelengths λ_k, $k=1, 2, 3$, and three canopy structure specific parameters. Denoting $\omega(\lambda_k)$, $p_{t,BS}$, and $p_{i,BS}$ by ω_k, p_t, and p_i, respectively, solutions can be written as

$$\omega_2 = \frac{a_1}{a_1-a_2} + \frac{a_1 a_2(1-k)}{k(1-q_t)(a_1-a_2)} + \frac{a_2}{a_1(1-k)}, \quad (A.2)$$

$$\omega_1 = k\omega_2, \quad (A.3)$$

$$p_i = \frac{a_2-(1-\omega_2)(1-q_t)}{a_2\omega_2}, \quad (A.4)$$

$$p_t = \frac{t_2-q_t}{\omega_2 t_2}, \quad (A.5)$$

$$\omega_3 = \frac{t_3-q_t}{t_3 p_t}, \quad (A.6)$$

where

$$k = \frac{(q_t-t_1)t_2}{(q_t-t_2)t_1}.$$

The portion of uncollided radiation in the total incident radiation q_t satisfies the following quadratic equation $b_2 q_t^2 + b_1 q_t + b_0 = 0$ where

$$b_2 = (t_2-t_1) + \gamma(t_1-t_3),$$

$$b_1 = (t_1-t_2)(1+t_3-a_2) + \gamma(t_3-t_1)(1+t_2-a_3),$$

$$b_0 = t_3(t_1-t_2)(a_2-1) + \gamma t_2(t_3-t_1)(a_3-1),$$

$$\gamma = \frac{a_2-a_1}{a_3-a_1}.$$

Its solutions can be expressed as

$$q_t = \frac{-b_1 \pm \sqrt{b_1^2-4b_0 b_2}}{2b_2}. \quad (A.7)$$

Values of q_t from the interval [0,1] are taken as solutions to the quadratic equation.

References

Baret, F., & Jacquemoud, S. (1994). Modeling canopy spectral properties to retrieve biophysical and biochemical characteristics. In J. Hill, & J. Megier (Eds.), *Imaging spectrometry—a tool for environmental observations* (pp. 145–167). Dordrecht, The Netherlands: Kluwer.

Bell, G. I., & Glasstone, S. (1970). *Nuclear reactor theory* (p. 619). New York: Van Nostrand Reinholt.

Blackburn, G. A. (1998). Quantifying chlorophylls and carotenoids at leaf can canopy scales: an evaluation of some hyperspectral approaches. *Remote Sensing Reviews*, *66*, 273–285.

Bonan, G. B. (1996). *A Land Surface Model (LSM version 1.0) for ecological, hydrological, and atmospheric studies*. Technical Description and user's guide, NCAR/TN-417+STR (pp. 88–102).

Box, M. A., Gerstl, S. A. W., & Simmer, C. (1988). Application of the adjoint formulation of the calculation of atmospheric radiative effects. *Beiträge zur Physik der Atmosphäre*, *61*, 303–311.

Broge, N. H., & Leblanc, E. (2000). Comparing prediction power and stability of broadband and hyperspectral vegetation indices for estimation of green leaf area index and canopy chlorophyll density. *Remote Sensing Reviews*, *76*, 156–172.

Bronshtein, I. N., & Semendyayev, K. A. (1985). *Handbook of mathematics* (p. 973). Berlin: Springer.

Buermann, W., Dong, J., Zeng, X., Myneni, R. B., & Dickinson, R. E. (2001). Evaluation of the utility of satellite-based vegetation leaf area index data for climate simulations. *Journal of Climate*, *14*, 3536–3550.

Chandrasekhar, S. (1950). *Radiative transfer* (p. 393). Oxford Univ. Press (reprinted, New York, NY: Dover, 1960) Oxford, UK.

Dickinson, R. E., Henderson-sellers, A., Kennedy, P. J., & Wilson, M. F. (1986). *Biosphere–atmosphere transfer scheme (BATS) for the NCAR*

Community Climate Model, Tech. Note TN-275+STR (p. 72). Boulder, CO, USA: National Center for Atmospheric Research.

Foley, J. A., Levis, S., Prentice, I. C., Pollard, D., & Thompson, S. L. (1998). Coupling dynamic models of climate and vegetation. *Global Change Biology*, *4*, 561–579.

Ioltukhovski, A. A. (1999). Radiative transfer over the surface with an arbitrary reflection: green's functions method. *Transport Theory and Statistical Physics*, *28*(4), 349–368.

Knyazikhin, Y., & Marshak, A. (2000). Mathematical aspects of BRDF modelling: adjoint problem and Green's function. *Remote Sensing Reviews*, *18*, 263–280.

Knyazikhin, Y., Martonchik, J. V., Myneni, R. B., Diner, D. J., & Runing, S. (1998). Synergistic algorithm for estimating vegetation canopy leaf area index and fraction of absorbed photosynthetically active radiation from MODIS and MISR data. *Journal of Geophysical Research*, *103*, 32257–32275.

Knyazikhin, Y., Mieben, G., Panfyorov, O., & Gravenhorst, G. (1997). Small-scale study of three dimensional distribution of photosynthetically active radiation in forest. *Agricultural and Forest Meteorology*, *88*, 215–239.

Lewis, M., Jooste, V., & de Gasparis, A. A. (2001). Discrimination of arid vegetation with airborne multispectral scanner hyperspectral imagery. *IEEE Transactions on Geoscience and Remote Sensing*, *39*, 1471–1479.

Li-COR (1992). *LAI-2000 plant canopy analyzer instruction manual* (pp. 4–12). Lincoln, NE, USA: Li-COR.

Martonchik, J. V., Diner, D. J., Kahn, R., Ackerman, T. P., Verstraete, M. M., Pinty, B., & Gorbon, H. R. (1998). Techniques for the retrieval of aerosol properties over land and ocean using multiangle imaging. *IEEE Transactions on Geoscience and Remote Sensing*, *36*, 1212–1227.

Myneni, R. B. (1991). Modeling radiative transfer and photosynthesis in three-dimensional vegetation canopies. *Agricultural and Forest Meteorology*, *55*, 323–344.

Panferov, O., Knyazikhin, Y., Myneni, R. B., Szarzynski, J., Englwald, S., Schnitzler, K. G., & Gravenhorst, G. (2001). The role of canopy structure in the spectral variation of transmission and absorption of solar radiation in vegetation canopies. *IEEE Transactions on Geoscience and Remote Sensing*, *39*, 241–253.

Pielke, R. A., Avissar, R., Raupach, M., Dolman, A. J., Xeng, Y., & Denning, S. (1998). Interactions between the atmosphere and terrestrial ecosystems: influence on weather and climate. *Global Change Biology*, *4,* 461–475.

Ross, J. (1981). The radiation regime and architecture of plant stands. Norwell, MA: Dr. W. Junk.

Sellers, P. J., Randall, D. A., Betts, A. K., Hall, F. G., Berry, J. A., Collatz, G. J., Denning, A. S., Mooney, H. A., Nobre, C. A., Sato, N., Field, C. B., & Henderson-sellers, A. (1997). Modeling the exchanges of energy, water, and carbon between continents and the atmosphere. *Science*, *275*, 502–509.

Serpico, S. B., & Bruzzone, L. (2001). A new search algorithm feature selection in hyperspectral remote sensing images. *IEEE Transactions on Geoscience and Remote Sensing*, *39*, 1360–1367.

Shabanov, N. V., Wang, Y., Buermann, W., Dong, J., Hoffman, S., Smith, G. R., Tian, Y., Knyazikhin, Y., Gower, S. T., Myneni, R. B. (2002). *Validation of the radiative transfer principles of the MODIS LAI/FPAR algorithm with data from the Harvard Forest*. Remote Sensing of Environment (in press).

Stamnes, K. (1982). Reflection and transmission by a vertically inhomogeneous planetary atmosphere. *Planetary and Space Science*, *30*, 727–732.

Thenkabail, P., Smith, R. B., & Paue, E. D. (2000). Hyperspectral vegetation indices and their relationships with agricultural crop characteristics. *Remote Sensing Reviews*, *71*, 158–182.

Tian, Y., Wang, Y., Zhang, Y., Knyazikhin, Y., Bogaert, J., & Myneni, R. B. (2001). Radiative transfer based scaling of LAI/FPAR retrievals from reflectance data of different resolutions. *Remote Sensing of Environment*, *84*, 143–159.

Van de Hulst, H. C. (1981). *Light scattering by small particles* (p. 470). New York: Dover Publications.

Zarco-Tejada, P. J., Miller, J. R., Mohammed, G. H., & Noland, T. L. (2000). Chlorophyll fluorescence effects on vegetation apparent reflectance: I. Leaf-level measurements and model simulation. *Remote Sensing of Environment*, *74*, 582–595.

Zarco-Tejada, P. J., Miller, J. R., Noland, T. L., Mohammed, G. H., & Sampson, P. H. (2001). Scaling up and model inversion methods with narrow band optical indices for chlorophyll content estimation in closed forest canopies with hyperspectral data. *IEEE Transactions on Geoscience and Remote Sensing*, *39*, 1491–1507.

Zhang, Y., Shabanov, N., Knyazikhin, Y., & Myneni, R. B. (2002). Assessing the information content of multiangle satellite data for mapping biomes: II. Theory. *Remote Sensing of Environment*, *80*, 435–446.

Zhang, Y., Tian, Y., Myneni, R. B., Knyazikhin, Y., & Woodcock, C. E. (2002). Assessing the information content of multiangle satellite data for mapping biomes: I. Statistical analysis. *Remote Sensing of Environment*, *80*, 418–434.